

High Voltage STM Imaging of Single Copper Phthalocyanine

C. Manzano, W.-H. Soe and C. Joachim

Abstract In this chapter experiments done to investigate the scanning tunneling microscope (STM) imaging at near field emission voltages of single Copper Phthalocyanine (CuPc) molecules deposited on Au(111) are presented. An imaging bias voltage range is explored exceeding the standard tunneling imaging conditions going from the threshold of the tunneling junction barrier up to -10.0 V. At this voltage regime current transmitted through the tip-molecule-substrate junction is made not only of tunneling electrons but also of electrons overcoming the tunneling barrier and behaving like free electrons. Our interpretation of the process, enabling the visualization of the electronic cloud of single organic molecules under these conditions, is presented.

1 Introduction

In [Chap. 1](#) the *far field* electron emission imaging technique known as Field Emission Microscopy (FEM) [1] was thoroughly described. The possibility of imaging molecules in real space is, however, not only restricted to the use of high electric fields. In a Scanning Tunneling Microscope (STM) bias voltages of a few volts (± 2.0 V) giving access to electronic states near the substrate's Fermi level are normally used to take images of low-resistance surfaces and molecules or adsorbates deposited on them.

C. Manzano (✉) · W.-H. Soe
IMRE, Agency for Science, Technology and Research (A*STAR), 3 Research Link 117602
Singapore, Singapore
e-mail: garciac@a-star.edu.sg

C. Joachim
CEMES/CNRS, Pico Lab, 29 Rue Marvig, BP 94347 31055 Toulouse Cedex, France

In a STM, the near field optics element of the microscope is a metal probe which is brought in close proximity, down to few angstroms, to a conductive surface until a current passing through the sample and tip, due to an applied bias voltage between them, set as a control parameter is measured. This current which passes through a potential barrier, whose width is determined by the tip-sample distance separation, is known as the tunneling current and is named after the quantum tunneling effect making possible its occurrence. Normally, an image of a selected substrate and adsorbates is obtained by scanning the tip above the substrate surface using an active feedback loop while applying voltages in between the sample and STM tip of a few volts (± 2.0 V). In this research work, we have gone further and explored whether it is possible to image single molecules beyond the typical voltage range (± 2.0 V) of standard tunneling STM imaging conditions by using even higher voltages exceeding the work function of either the tungsten STM tip or the Au(111) crystal used as a substrate in these experiments. STM images acquired under these conditions are considered to be taken in the *near field emission regime*.

For using FEM to image organic molecules, the appropriate trade-off between FEM's operation parameters, i.e., emission voltage and electrode-screen distance, needs to be determined and set in order to preserve the integrity of the metal tip electrode as well as to avoid breaking the molecule to be observed. For that purpose, voltages below the metal tip breakdown voltage [2] are selected in combination with the tip-screen distance, with values falling within the area below the voltage breakdown curve shown in Fig. 1, to concurrently keep the molecule undamaged and obtain the best molecule image resolution. Actually, by decreasing these parameters down to their lowest limit, so that the voltage in between the FEM electrodes is of few volts and their distance separation is of few angstroms, we would end up with an experimental conformation resembling an STM. Likewise, an STM tunneling junction can be considered the analog of a FEM setup with the scanning STM tip functioning as a mobile single pixel screen and the sample acting as the emitting electrode. In principle, by using the appropriate experimental parameters, i.e., tip-sample distance and high enough voltages, an STM should be able to image in the near field emission mode.

Low voltage (± 2.0 V) imaging parameters are standard and commonly used in STM-based investigations. On the contrary, STM imaging in the near field emission regime has been less explored. Early STM electron spectroscopy experiments investigating conductance spectra taken using voltages within the near field emission regime showed the existence of distinctively spaced resonances in the electron spectra [3–5]. These resonances were previously predicted by Gundlach [6] and are thought to arise due to resonant tunneling through electronic states resulting from a Fabry–Perot cavity confinement, formed by the asymmetric energy potential formed in the tunneling junction produced by the high electric fields applied in between the electrodes, see Fig. 2.

The existence of these high differential conductance Gundlach resonances, also known as field emission resonances (FER), has made possible to STM image large wide gap semiconductor surfaces like C(001) [7] whose energy band gap is

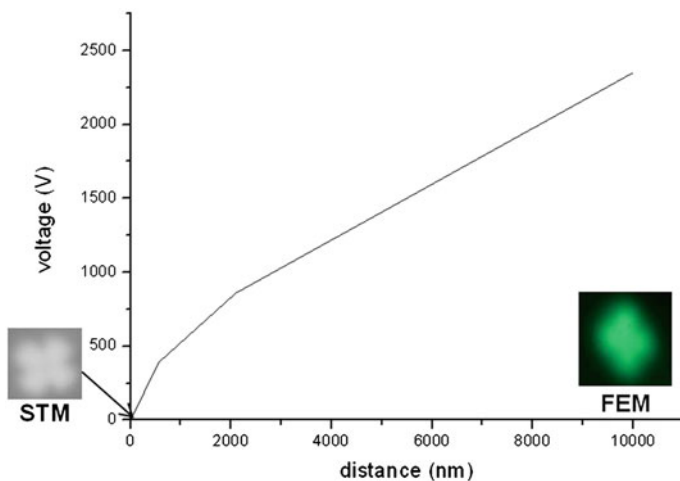


Fig. 1 Breakdown voltage curve showing the maximum voltage that can be applied between FEM electrodes at a given electrode distance separation before any of them gets damaged. For single molecule, FEM imaging the best trade-off between voltages in the area below this curve and the electrodes distance is selected to ensure that electrodes and molecules remain undamaged and to get the best image resolution. In principle, by setting the appropriate parameters it would be possible to get images using field emission electrodes in the far and near fields with either a FEM or an STM. Images of single CuPc taken using FEM and STM at these different imaging regimes are also shown (CuPc FEM image courtesy of Mohamed Rezeq)

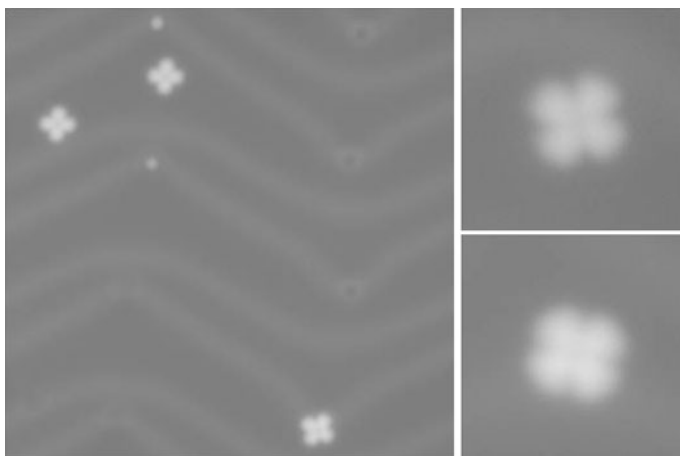


Fig. 2 Topographic STM image showing single CuPc molecules deposited on Au(111), the characteristic “herringbone” surface reconstruction of Au(111) is also observed (image size: 24×24 nm). The top and bottom images at the left correspond to CuPc molecule images taken at -2.0 and 2.0 V, respectively (image size: 4.5×4.5 nm)

~ 7.0 V. Carbon dimer lines of the topmost layer of a diamond surface are imaged with near atomic resolution by setting the STM bias voltage at the value corresponding to the first resonance maxima in C(001) dZ/dV spectra, which is above the C(001) conduction band edge. The same FER imaging approach has also been used to investigate the dynamics of surface electrons in metal surfaces and alkali metal clusters [8, 9]. We are not aware of any research work intentionally targeting the FER imaging of single molecules.

To explore the STM imaging of single molecules, through the whole voltage range, the model molecule CuPc was selected. An Au(111) crystal was used as a substrate in these experiments since it has been already reported that CuPc as well as other molecules like Pentacene and Starphene upon sublimation on Au(111) are physisorbed [10]. Likewise, CuPc adsorption state on Au(111) results in electronically weakly coupled CuPc molecules, whose electronic structure is minimally modified and allows at the same time access to well-separated electronic resonances in the transmission spectra of the tunnel junction.

A submonolayer of CuPc molecules was deposited on a clean Au(111) crystal via free evaporation from a quartz crucible heated to 623 K with the Au(111) substrate held at ~ 473 K. Thereafter, the sample was cooled down with liquid helium and transferred to the STM system. Before the molecule deposition the substrate was cleaned after undergoing several cycles of sputtering and annealing. All the STM experiments were done using a Createc low temperature STM operating at a base pressure of at least 8×10^{-11} mbar and ~ 7 K. Standard tunneling spectroscopy methods were also used to measure differential conductance (dI/dV) spectra.

2 Experiments and Results

STM images taken after CuPc/Au(111) sample preparation show that CuPc molecules adsorbed on terraces and also at step edges, see Fig. 2, the characteristic surface reconstruction of Au(111) is also observed. In low voltage STM topographic images of isolated single CuPc molecules taken using voltages from +2.0 to -2.0 V, a CuPc appears like a symmetric four-lobed cross without any intramolecular features being discernible, characteristic images taken within that range are shown in Fig. 2. A comprehensive analysis of CuPc molecular electronic states, upon adsorption on Au(111), was done by measuring the tunneling junction transmission resonances using tunneling spectroscopy and also by mapping the differential conductance at selected voltages. The results and findings of that investigation are reported in another chapter of this book.

So far, we have shown STM images taken with bias voltages set within standard imaging conditions characteristic of the tunneling regime (± 2.0 V) in which the whole current passing through the tip and sample is made of tunneling electrons, as shown in the diagram in Fig. 3. These imaging parameters are standard and commonly used in STM-based investigations.

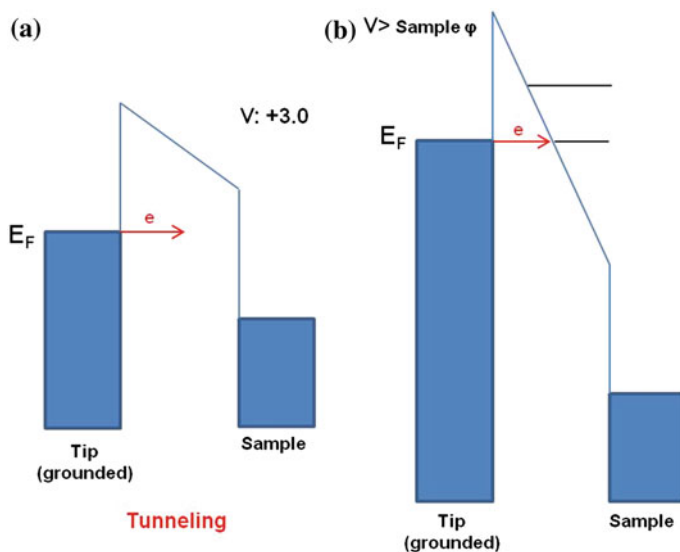


Fig. 3 **a** Schematics showing the electron tunneling through a potential barrier from the STM tip to the sample for standard tunneling bias conditions. **b** Potential barrier diagram showing the existence of electron confinement due to the potential deformation resulting from applying voltages within the STM junction above the sample's work function. Resonant tunneling through the electronic states in the near field emission regime gives rise to Gundlach resonances observed in the dZ/dV spectra

After getting images and dI/dV maps of CuPc using parameters considered to be within the standard tunneling conditions, we proceeded to take images at higher positive and negative voltages with the aim of finding out whether it is possible to image single CuPc molecules using FER imaging without breaking them. The voltage range explored in our investigation is constrained to the maximum voltage range (± 10 V) attainable by the digital analog converters of the electronic system used to operate our STM instrument.

Z/V and dZ/dV spectra are taken on a bare Au(111) terrace to determine the spectral position of the Gundlach resonances in the tip-substrate tunneling junction used in these experiments, shown in Fig. 4. The spectra are taken with the STM feedback loop active, so that the tunneling current stays constant while a voltage ramp is applied. Because the feedback loop is "ON", the STM piezo tube holding the STM tip adjusts the tip-sample distance or tip height displacements Z to keep the tunneling current constant at the value initially set as a control parameter; the changes in Z are recorded in function of the voltage applied giving rise to the Z/V while concurrently using a lock-in amplifier to obtain the dZ/dV spectra. Both type of spectra recorded at positive voltages present the characteristic high voltage resonances previously observed in other systems. Interestingly, these spectra are easily reproduced regardless of whether the STM tip is fit enough for getting topographic images or not.

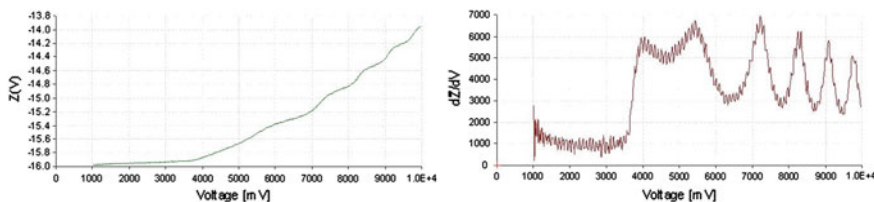


Fig. 4 Z/V and dZ/dV spectra taken at positive voltages from 1.0 to 10.0 V on a bare Au(111) terrace. Both spectra show the existence of Gundlach resonances in the tip-substrate tunneling junction used in these experiments. The spectral position of the resonances was used as a reference in the near field STM imaging of CuPc

After confirming that we are able to identify Gundlach resonances, a sequence of topographic images shown in Fig. 5 was taken starting from 2.5 V and gradually increasing the bias voltage up to about 6.0 V to visualize the CuPc molecule before and after the abrupt differential conductance step-like increase in the dZ/dV in Fig. 4, taking place in between the 3.0 and 4.0 V range. The characteristic cross shape of CuPc is clearly seen at 2.5 V; however, in images taken at about 3.0 V the four lobes become indistinguishable and the molecules are imaged as bright blobs where the molecule's inner structure cannot be recognized. At 4.0 V, already at voltages where tunneling conductance shows a drastic increase in the dZ/dV, a CuPc molecule appears having a bright four-peaked star-like shaped center with four dimmer lobes in between the star peaks. Comparing with CuPc images taken at lower voltages reveals that all features captured at 4.0 V are rotated 45° with respect to the cross-shaped CuPc images; the four peaks of the star-like center appear to arise from the areas in between the lobes of CuPc. When images are taken at 4.6 and 5.5 V which correspond, respectively, to an anti-resonance and a resonance peak in the dZ/dV, the star shape and all other intramolecular features previously observed appear broadened and cannot be easily identified anymore, blurring and overshadowing the overall molecule shape observed at low voltages. Attempts to image CuPc at even slightly higher voltages damaged the molecules as is shown in the last image of Fig. 5, which was taken after trying to image scanning at 6.0 V. The fragmentation of CuPc at these relatively low voltages hindered the realization of further experiments to FER imaging CuPc at the voltages corresponding to the four topmost high voltage resonances appearing in the dZ/dV above 7.0 V in Fig. 4.

Thereafter, the same approach was followed using negative polarity voltages, characteristic Z/V, and dZ/dV spectra taken on a bare Au(111) as shown in Fig. 6. Contrary to spectra taken at positive biases these spectra do not present any sign of Gundlach resonances. It is worth to notice that Gundlach resonances have been observed only in tip-substrate junctions using positive voltage polarities where electrons are emitted and transmitted from the STM tip to the sample. We think that, the absence of Gundlach resonances at negative voltages where electrons move from the sample to the tip is a consequence of the different asymmetric spatial confinement experienced by the emitted electrons, depending on whether

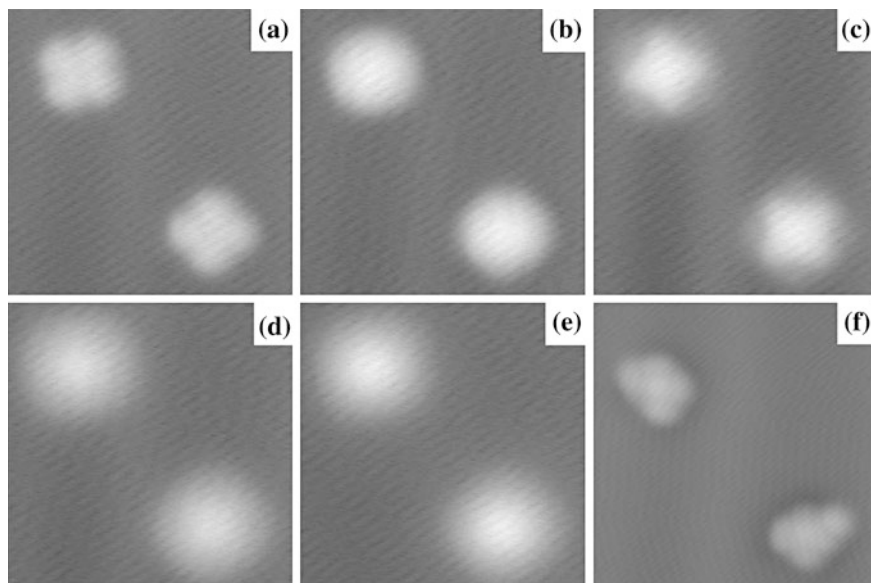


Fig. 5 Sequence of CuPc's STM images taken at positive voltages. **a** The characteristic cross shape of CuPc is clearly seen at 2.5 V. **b** At about 3.0 V, the molecules are imaged as bright blobs where the molecule's inner structure cannot be recognized anymore. **c** At 4.0 V, CuPc appears having a star-like shaped center with four dimmer lobes in between the four star peaks. **d** and **e** Images are taken at 4.6 and 5.5 V, they correspond, respectively, to an anti-resonance and a resonance peak in the dZ/dV , all intramolecular features previously observed appear broadened, blurring, and overshadowing the overall molecule shape observed at low voltages. **f** CuPc molecules damaged after trying to image them scanning at 6.0 V (image size: 6.7×6.7 nm)

they are transmitted from the tip to the sample or from the sample to the tip. At positive voltages, the emitted electrons move from the tip toward a planar electrode to the substrate's surface, such tunneling junction acts as an effective Fabry–perot-like cavity giving rise to well-separated electron states. On the contrary, at negative polarities electrons emitted from the sample are transmitted to the tip—a non-planar electrode resulting in a tunneling junction less effective as a cavity and

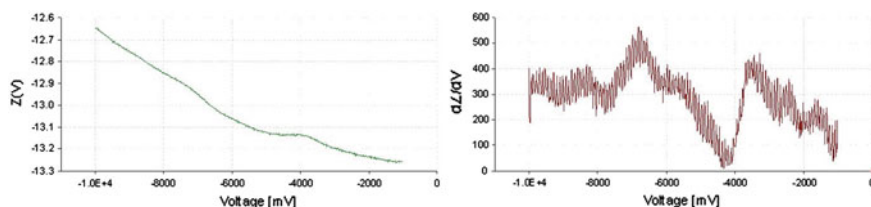


Fig. 6 Z/V and dZ/dV spectra taken at negative voltages from -1.0 to -10.0 V on a bare Au(111) terrace. Contrary to spectra taken at positive voltages these spectra do not show any trace of the Gundlach resonances

where confinement of the electrons leaving the metal substrate does not take place, as evidenced in the dZ/dV spectra.

In spite of the absence of Gundlach resonances in the dZ/dV spectra, we proceeded to image CuPc at voltages above the tungsten tip work function; the sequence of images taken from -3.0 V up to -10.0 V is shown in Fig. 7. In the images taken using low voltages going from -3.0 V up to -5.0 V, the already well-known characteristic shape of CuPc is visualized, while images taken at higher voltages all the way up to -10.0 V become gradually blurry concomitantly with the voltage rise. Moreover, the images lose resolution, the inner molecule features observed at lower voltages are blurred, and CuPc's four lobes appear broadened making the space in between them undistinguishable. At -10.0 the CuPc image does not resemble anymore the cross-like shape observed at low voltages. What is remarkable, however, is that after this image sequence was taken the CuPc molecule integrity is preserved.

High voltage imaging at negative bias was also done on single Azastarphene molecules deposited on Au(111) showing similar results (see Fig. 8). STM images obtained using tunneling regime parameters show Azastarphene like a three-peaked star-shaped molecule. High voltage images obtained at -9.0 and -10.0 V show likewise in the case of CuPc lower resolution. The three branches of Azastarphene appear broadened and submolecular features that are clearly visible in low voltage images are completely blurred.

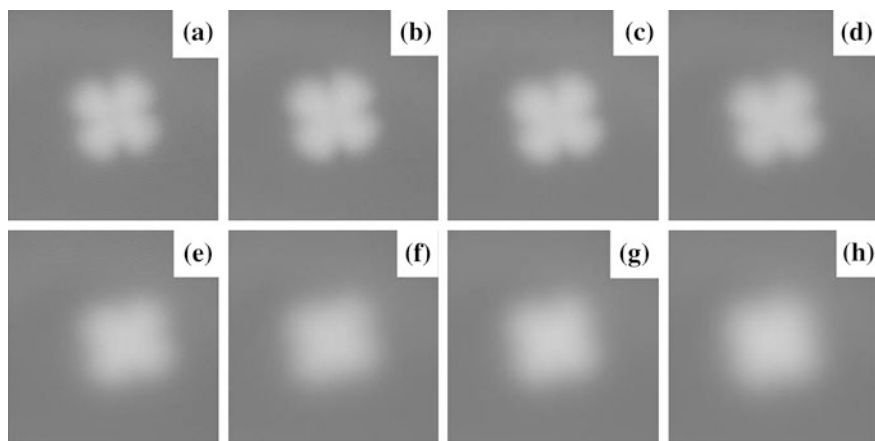


Fig. 7 Sequence of CuPc's STM images taken at negative voltages. *Top row images (a–d)* were taken at -3.0 , -4.0 , -5.0 and -6 V, respectively, the characteristic four lobed crossed-like shape of CuPc is visualized. *Bottom row images (e–h)*, taken at -7.0 , -8.0 , -9.0 and -10.0 V become gradually blurry. CuPc's intramolecular resolution decreases and its four lobes appear broadened making the space in between them undistinguishable (image size: 4.5×4.5 nm)

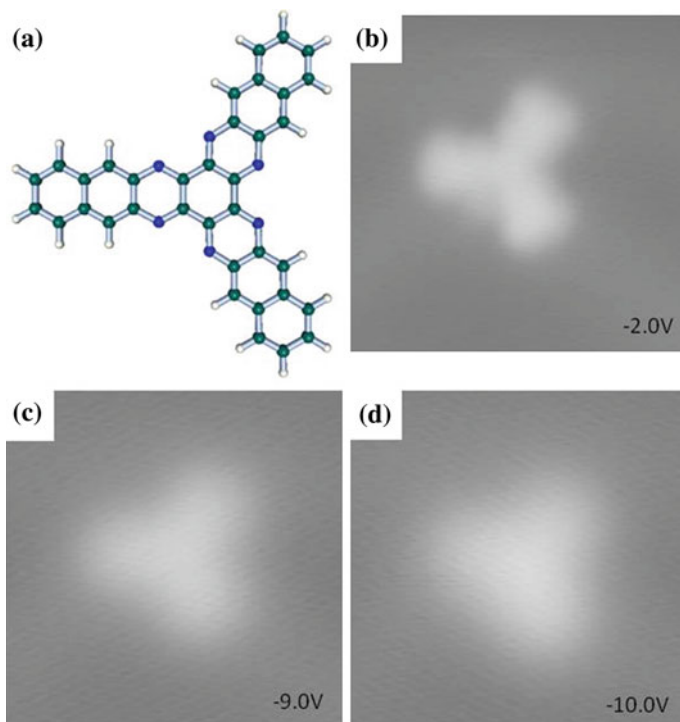


Fig. 8 **a** Ball and stick model of the Azastarphene molecule. **b** STM image of Azastarphene taken using standard tunneling imaging parameters **(c)** and **(d)** are images taken in the near field emission regimen, the three lobes of Azastarphene appear broaden and submolecular features in the branches that are clearly visible in low voltage images are completely blurred (image size: 4.5×4.5 nm)

3 Interpretation

To understand and explain the gradual contrast and resolution changes taking place during STM-near field emission imaging, we need to revisit a well-known effect in the wave optics field, the diffraction effect occurring when an optic wave travels through a circular aperture or a pinhole. The wave planes of an incident light beam passing through a circular aperture will be diffracted depending on the aperture diameter and wavelength of the incoming wave. The diffracted wave can be imaged by placing a recording media or screen in front of the aperture. The diffraction due to a circular aperture will form a two-dimensional pattern made of a central bright spot known as Arago spot and evanescent concentric ridges (Fig. 9) [11].

Diffracted waves also broaden spatially when moving and spreading away from the aperture [11], the pattern spatial spreading (W) captured by a screen position at a given distance (X) from the aperture depends on several parameters like the wavelength of the incoming wave planes, the aperture diameter (a), and the screen

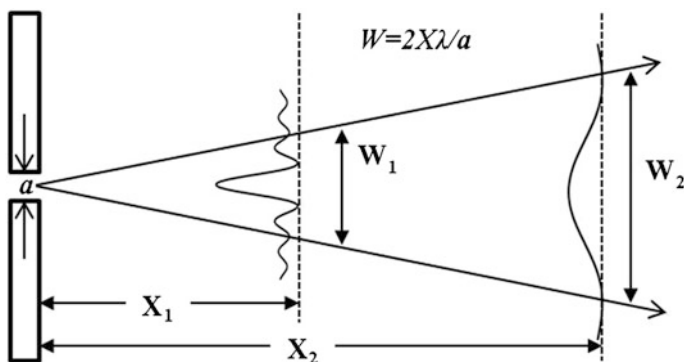


Fig. 9 Sketch showing how diffracted waves broaden spatially, when they spread away from an aperture. The cross-section of the diffraction pattern recorded at two different distances from the aperture shows the diffraction pattern broadening and its intensity attenuation

distance from the aperture (X) and can be approximated by the expression $W = 2X\lambda/a$. An example showing how the diffraction pattern spreads away from the aperture is shown in Fig. 9. The cross-section broadening of the diffraction pattern due to a circular aperture recorded at two different distances is also shown.

Evidently, there is not an actual aperture in the Au(111) surface, however, a molecule adsorbed on the metal substrate modifies locally the substrate's work function lowering the tunneling barrier height [12]. The perturbation of the barrier renders an area with the shape and footprint of the CuPc with a lower barrier height relative to that of Au(111) and in analogy to light waves passing through an aperture the STM tip will detect field emitted electrons passing through an "aperture", whose shape is defined by the CuPc molecule.

The whole sequence of CuPc high voltage images was taken using the constant current mode and as shown before in the $Z(V)$ in Fig. 6 when the feedback loop is active the tip height is adjusted by the STM electronics to keep the current constant; the $Z(V)$ shows that the tip moves away from the substrate commensurately with the voltage. Consequently, CuPc images in that sequence taken at increasing voltages were accordingly also taken at increasing larger tip-molecule distances relative to each other. The blurring and broadening present in the CuPc near field emission images, shown in Fig. 7, are the effects of retracting the STM tip *screen* away from the *aperture* and the sample surface by subsequently increasing the imaging voltage. This is a pure optics-like effect due to the field emitted electrons passing through the CuPc "aperture" that is made more evident by moving the *screen* away from the electrons source.

This hypothesis is reinforced by taking two series of images at tunneling resistances resulting in two image sets, which are shown in Fig. 10, obtained at different tip-substrate distances. By comparing the two series of near field emission images, it can be clearly noticed that the CuPc images taken at the same voltage but larger tip-substrate distances have lower resolution and appear blurred and

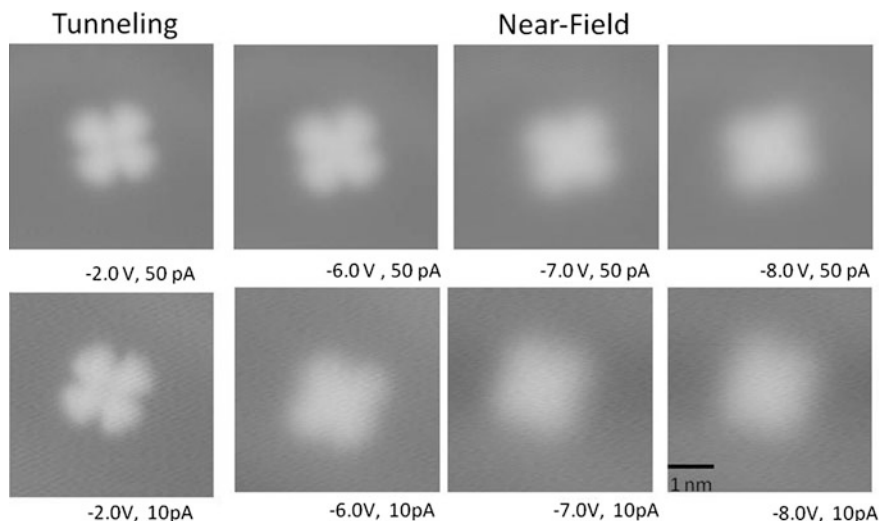


Fig. 10 Sequences of STM images taken at tunneling resistances resulting in two image sets obtained at different tip-substrate distances. The near field emission images show clearly that the CuPc images taken at the same voltage but larger tip-substrate distances have lower resolution and appear blurred and broadened relative to those taken at shorter distances. The images taken using standard tunneling parameters show that the two different tip-substrate distances have no effect in terms of image resolution (image size: 4.5×4.5 nm)

broadened relative to those taken at shorter distances. That optics-like blurring and broadening is only observed in images taken in the near field regime at which STM images are made of the superposition of contributions due to tunneling electrons and field emitted electrons. As shown in the leftmost images in Fig. 10, it is clear that for images taken using low voltages at which the transmitted current through the tunneling junction is made of only tunneling electrons—the two different tip-substrate distances have no effect in terms of image resolution.

4 Conclusion

Low temperature STM experiments were done to investigate the possibility of imaging single CuPc molecules deposited on Au(111) using parameters that exceed the standard ones normally used for STM imaging and lie within the near field emission range. The imaging of single CuPc and Trianthracene molecules using voltages above the tip work function demonstrate that it is possible to use STM near field emission at negative bias voltages without damaging the target molecules.

The blurring and broadening of intramolecular features observed in images taken in the near field emission is analogous to the diffraction pattern broadening

observed when the diffraction pattern of a light beam passing through a circular aperture spreads away from the aperture. STM near field emission images are made of the superposition of contributions to the measured current due to both tunneling electrons and field emitted electrons. The weight of field emitted electrons contribution showing up in the images as optic-like blurring and broadening will depend not only on the imaging bias voltage but also on the tip-sample distance.

Acknowledgments We acknowledge financial support from the Agency of Science, Technology, and Research (A*STAR) for the Visiting Investigatorship Program (Phase III): AtomTech Project and the European Commission integrated project AtMol.

References

1. Melmed, A.J., Muller, E.W.: Study of molecular patterns in the field emission microscope. *J. Chem. Phys.* **29**, 1037 (1958). doi:[10.1063/1.1744651](https://doi.org/10.1063/1.1744651)
2. Boyle, W.S., Kisliuk, P., Germer, L.H.: Electrical breakdown in vacuum. *J. Appl. Phys.* **26**, 720 (1955). doi:[10.1063/1.1722078](https://doi.org/10.1063/1.1722078)
3. Binnig, G., Frank, K.H., Fuchs, H., Garcia, N., Reihl, B., Rohrer, H., Salvan, F., Williams, A.R.: Tunneling spectroscopy and inverse photoemission: image and field states. *Phys. Rev. Lett.* **55**, 991 (1985). doi:[10.1103/PhysRevLett.55.991](https://doi.org/10.1103/PhysRevLett.55.991)
4. Becker, R.S., Golovchenko, J.A., Swartzentruber, B.S.: Electron interferometry at crystal surfaces. *Phys. Rev. Lett.* **55**, 987 (1985). doi:[10.1103/PhysRevLett.55.987](https://doi.org/10.1103/PhysRevLett.55.987)
5. Kubby, J.A., Wang, Y.R., Greene, W.J.: Fabry-Perot transmission resonances in tunneling microscopy. *Phys. Rev. B* **43**, 9346 (1991). doi:[10.1103/PhysRevB.43.9346](https://doi.org/10.1103/PhysRevB.43.9346)
6. Gundlach, K.H.: Zur Berechnung des Tunnelstroms Durch eine Trapezförmige Potentialstufe. *Solid State Electron.* **9**, 946 (1966). doi:[10.1016/0038-1101\(66\)90071-2](https://doi.org/10.1016/0038-1101(66)90071-2)
7. Bobrov, K., Mayne, A.J., Dujardin, G.: Atomic-scale imaging of insulating diamond through resonant electron injection. *Nature* **413**, 616 (2001). doi:[10.1038/35098053](https://doi.org/10.1038/35098053)
8. Pascual, J.I., Corriol, C., Ceballos, G., Aldazabal, I., Rust, H.-P., Horn, K., Pitarke, J.M., Echenique, P.M., Arnau, A.: Role of the electric field in surface electron dynamics above the vacuum level. *Phys. Rev. B* **75**, 165326 (2007). doi:[10.1103/PhysRevB.75.165326](https://doi.org/10.1103/PhysRevB.75.165326)
9. Stepanow, S., Mugarza, A., Ceballos, G., Gambardella, P., Aldazabal, I., Borisov, A.G., Arnau, A.: Localization, splitting, and mixing of field emission resonances induced by alkali metal clusters on Cu (100). *Phys. Rev. B* **83**, 115101 (2011). doi:[10.1103/PhysRevB.83.115101](https://doi.org/10.1103/PhysRevB.83.115101)
10. Soe, W.-H., Manzano, C., De Sarkar, A., Chandrasekhar, N., Joachim, C.: Direct observation of molecular orbitals of pentacene physisorbed on Au (111) by scanning tunneling microscope. *Phys. Rev. Lett.* **102**, 176102 (2009). doi:[10.1103/PhysRevLett.102.176102](https://doi.org/10.1103/PhysRevLett.102.176102)
11. Pedrotti, F.L., Pedrotti, L.S., Pedrotti, L.M.: Introduction to Optics, 3rd edn. Addison-Wesley, Reading (2006)
12. Wu, S.W., Ogawa, N., Nazin, G.V., Ho, W.: Conductance hysteresis and switching in a single-molecule junction. *J. Phys. Chem. C* **112**, 5241 (2008). doi:[10.1021/jp7114548](https://doi.org/10.1021/jp7114548)

Imaging and Manipulating Molecular Orbitals

Proceedings of the 3rd AtMol International Workshop,
Berlin 24-25 September 2012

Grill, L.; Joachim, C. (Eds.)

2013, VIII, 206 p. 97 illus., 84 illus. in color., Hardcover

ISBN: 978-3-642-38808-8